applied sciences

MDPI

Article

Evaluation of Cement Performance Using Industrial Byproducts Such as Nano MgO and Fly Ash from Greece

Panagiota P. Giannakopoulou [1], Aikaterini Rogkala [1], Paraskevi Lampropoulou [1], Maria Kalpogiannaki [1] and Petros Petrounias [1,2,*]

[1] Section of Earth Materials, Department of Geology, University of Patras, 26504 Patras, Greece; peny_giannakopoulou@windowslive.com (P.P.G.); k.rogkala@upatras.gr (A.R.); p.lampropoulou@upatras.gr (P.L.); maria.kalpogiannaki@gmail.com (M.K.)

[2] Centre for Research & Technology Hellas (CERTH), Chemical Process & Energy Resources Institute, Maroussi, 15125 Athens, Greece

* Correspondence: Geo.plan@outlook.com

Abstract: The need for environmentally friendly construction materials is growing more and more these days. This paper investigates byproducts from Greece, such as magnesite tailings from Evoia and fly ash from Kardia (Ptolemais), in order to evaluate their suitability as cement additives. For this purpose, the raw materials were tested and studied regarding their mineralogical and chemical components for their morphological characteristics. Different cement specimens of various mixtures of raw materials were produced and tested. These raw materials are considered suitable for cement additives. The effect of nano MgO content seems to have played a more critical role in the physicomechanical performance of produced cement compared to that of the fly ash content. Furthermore, more satisfactory results in the physicomechanical properties of the produced cement gave samples of group II containing 3–4% of nano MgO. Nano MgO content up to 4% seems to have negative influence on the compressive strength of the produced cement, simultaneously reducing its durability. The increase of nano MgO content leads to the increase of the expansion of the produced cement specimens. In the early stage, the expansion rate was intensively larger. With the consumption of nano MgO, the expansion in the later stage gradually slowed down and tended to stabilize.

Keywords: magnesite tailings; nano MgO; fly ash; cement

Citation: Giannakopoulou, P.P.; Rogkala, A.; Lampropoulou, P.; Kalpogiannaki, M.; Petrounias, P. Evaluation of Cement Performance Using Industrial Byproducts Such as Nano MgO and Fly Ash from Greece. *Appl. Sci.* **2021**, *11*, 11601. https://doi.org/10.3390/app112411601

Academic Editors: Carlos Morón Fernández and Daniel Ferrández Vega

Received: 22 October 2021
Accepted: 4 December 2021
Published: 7 December 2021

1. Introduction

Cement is widely used as a basic component of concrete. Due to the rapid construction development, the demand for cement and natural aggregates has, exceptionally, been increased. More specifically, in 2014, about 40 billion tons of aggregates and 4 billion tons of cement were required for constructions all over the world [1,2]. As a result, a great amount of carbon dioxide (CO_2) is released in the air. This is the reason why several researchers, i.e., [3,4], have turned their attention to producing environmentally friendly applications, and at the same time, they have reduced CO_2 emissions during their production. The reaction of cement and water produces volume shrinkage, which may lead to structural cracking of cement-based materials [5]. This is detrimental not only for the mechanical properties and durability of cement-based materials, but it may also lead to shorter service life of constructions, resulting in a great loss of natural resources. The problem of shrinkage of cement is becoming more and more serious, as by increasing the concrete strength, the amount of cement per unit volume of concrete increases, too [6,7]. Cementitious concrete is the most-used manmade material among all, and comprises a mixture of mortar, aggregates, and water [2,4,8]. The main component of concrete is the material which binds the aggregate particles together, commonly comprising a mixture of cement and water [4,8]. Concrete structures can be described as a three-phase system composed of hardened cement paste, aggregate, and the interface between aggregate particles and cement paste [8,9].

One of the effective ways to reduce cracking is by adding expansion agent in cement concrete or by using the expansion generated during the hydration process of expansion agent to compensate the shrinkage of cement concrete [5,6]. Nowadays, the expansion agents mainly used in several applications primarily include sulfoaluminate-type, CaO-type, and MgO-type expansion agents. In comparison with the first two kinds of expansion agents, MgO expansion agent (nano MgO) displays a lot of advantages, including less water requirement for hydration, stable hydration product $Mg(OH)_2$, adjustable design of expansion process, and so on, in order to widely to be used in modern concrete [10]. Since the 1970s, numerous researchers have begun to study MgO expansion agent (MEA), which has been applied to a wide range of buildings, such as dams. The expansion produced by MEA hydration is used to compensate the temperature drop shrinkage and dry shrinkage of mass concrete, effectively improving the crack resistance and durability of the structure [11,12].

Cements with high MgO content have gained more and more popularity in the last decade, perhaps due to the augmented concern about climate change, with the intention and need of reducing the CO_2 emissions regarding the production of conventional Portland cements. Some authors believe that it is possible to produce such type of cements with a high MgO content and reduced CO_2 emissions [13]. In recent decades, the major motivation for the development and uptake of MgO-based cements has been driven from an environmental standpoint. The lower temperatures required for the production of MgO compared to the conversion of $CaCO_3$ to PC and the energy savings associated with this reduced temperature have led researchers to envision MgO-based cements as being central to the future of ecofriendly cement production. Equally, the ability of MgO to absorb CO_2 from the atmosphere to form a range of carbonates and hydroxycarbonates lends itself well to the discussion of "carbon-neutral" cements, which could potentially absorb close to as much CO_2 during their service life as was emitted during their manufacture. These two interconnected aspects have led to a recent explosion in interest, both academic and commercial, in the area of MgO-based cements.

Magnesium is the eighth most abundant element in the Earth's crust, at ~2.3% by weight, present in a range of rock formations such as dolomite, magnesite, and silicate. Magnesium is also the third-most abundant element in solution in seawater, with concentrations of ~1300 ppm [5]. The mineral magnesite comprises a widely used source of magnesium oxide (MgO), because magnesium is considered a critical element by the EU. However, alternative sources, such as several Mg-rich silicates, may become more relevant in the near future. The transition of magnesite to magnesia has been achieved by heat treatment at temperatures above 600 °C. This transition from carbonate to oxide by release of carbon dioxide (CO_2) initially produces a porous microstructure with low bulk density. Moreover, this material is characterized as a strong reactive due to its low magnesia particle sizes with high surface areas which can be retained if not heated further. Such high surface area variants of magnesia are known as "active magnesia" in cement-related research. Exposing this porous form to higher temperatures (>1200 °C) solidifies the structure by a sintering mechanism and drastically reduces the reactive surface area as well as the affected sites that promote wetting and dissociation of magnesia in acid phosphate solutions. Magnesia-based cements, by definition, use MgO as a building block rather than the CaO which represents more than 60% of the elemental composition of PC. Due to the substantially different chemistry of MgO compared to that of CaO, one cannot simply change the feedstock for conventional Ca-based cements to produce a directly corresponding material using the same infrastructure. Comparing the respective (MgO, CaO)–Al_2O_3–SiO_2 ternary phase diagrams, vast differences in chemistry and phase formation are shown. More specifically, no magnesium silicate phases are formed in high temperatures that have hydraulic properties akin to those formed in the calcium-rich region of the CaO–SiO_2–Al_2O_3 system: Ca_3SiO_5, Ca_2SiO_4, and $Ca_3Al_2O_6$ are critical hydraulic phases in PC, but have no magnesian analogues.

Currently, the MEA used in the market is mainly produced by the calcining of magnesite. However, with the continuous mining of mineral resources, the problems of resource exhaustion and environmental pollution are becoming more and more threatening. Following governments' instructions regarding the mining of nonrenewable mineral resources, magnesite resources are decreasing [14] while, at the same time, a large amount of magnesite is discarded annually. These gradually accumulated large amounts of magnesite not only occupy cultivated land but also cause waste of resources. Magnesite is a raw material used in different industrial applications. It is used mainly after heat treatment for the production of caustic magnesia and dead burned magnesia, whilst untreated magnesite has a few industrial applications too (e.g., in the production of fertilizers, electrodes, and environmental protection). The main magnesite deposits in Greece appear in Chalkidiki and Evoia Island. Regarding the case of Evoia's magnesite deposits, they have been started to be exploited since 1893 mainly for the production of magnesia-rich raw materials and refractory final products. In this area, the proven, probable, and possible reserves have been approximately estimated as 35, 45, and 60 million tons, respectively [15]. The concession areas cover ~404 km^2 while all mines are within a 14 km radius around the refractory industry plants. The last is 2 km away from the loading port. According to the current activities, the annual capacity is 120,000 MT of caustic magnesia and dead burned magnesia, while above 250,000 tons of stockpile waste have been disposed of in the area during last year's activities. They consist of the fine ore (−40 mm) which is rejected before the beneficiation processing and specifically before the hand-sorting stage of magnesite. This tailing contains significant amounts of magnesite, and in this work, the feasibility of its utilization as MEA is studied. In the Greek market, materials of similar quality are found, but they are produced from natural mineral raw materials and not from byproducts.

The real contribution of such initiatives does not result in a notable decrease in negative externalities. This fact can be assigned to a limited acceptance of "greener" building materials [16]. The relatively poor adoption of modified binders represents a barrier towards a more sustainable construction industry [17]. However, the change of this paradigm needs to be completed not only by the technical parameters but also must be combined with other scientific disciplines involved in the sustainability principles [18]. In a nutshell, new design and development materials must go hand in hand with corresponding leadership, convincing communication, and complex assessment of ecofriendly materials to overcome major barriers in the conservative building industry. Numerous researchers who study green construction materials and applications often use micropetrographic analytical methods [19].

The aim of this study is to evaluate the impact of MEA combined with fly ash on final physicomechanical performance of the produced mortar, providing a new way to solve the environmental pollution of magnesite tailings and fly ashes. For this scope, magnesite tailings and fly ash from Greece were used where the influence of different percentages of MEA combined with fly ash on the physicomechanical performance of the produced cements were studied.

2. Geological Setting of Magnesite Tailings

Magnesite tailings are located in central and northern Evoia and are occupied by Jurassic ophiolitic rocks such as harzburgites and basalts (Figure 1). These rocks overlay a mélange (the Pagondas complex), comprising Upper Triassic to Jurassic sedimentary and volcanic rocks, which was developed as an accretionary prism [20]. The entire sequence of the ophiolitic rocks and the mélange is thrust on the Pelagonian carbonate platform. The ultramafic rocks are covered by Pliocene terrigenous and minor marine and lacustrine sediments, and Quaternary deposits [21]. The overthrust of the Evoia ophiolite is structurally overlain by a dismembered metamorphic sole which constitutes evidence for a late Upper Jurassic emplacement age [22,23]. Magnesite is presented as cryptocrystalline, mostly nodular, and appears as open space fillings along joints of ultramafic rocks, forming stockworks, as veins controlled by brittle faults, indicating that magnesite was deposited

during opening of the veins in an extensional geodynamic regime, and as nodular forms that resulted from replacement of ultramafic rock. Those nodules are mainly centimeter-sized and contain relics of chromite. Magnesite also predates deposition of dolomite and silica polymorphs where a vertical mineral zonation is evident: magnesite modal percentages decrease towards the surface, whereas dolomite and quartz gradually become more abundant. Moreover, vuggy silica textures are presented in the uppermost parts. Brecciation of early-formed magnesite and cementation by magnesite deposited at a later stage is also observed. Both the deposits of stockwork type of mineralization and the main veins have not been deformed. Significant displacements by younger faults affecting the deposits are not observed.

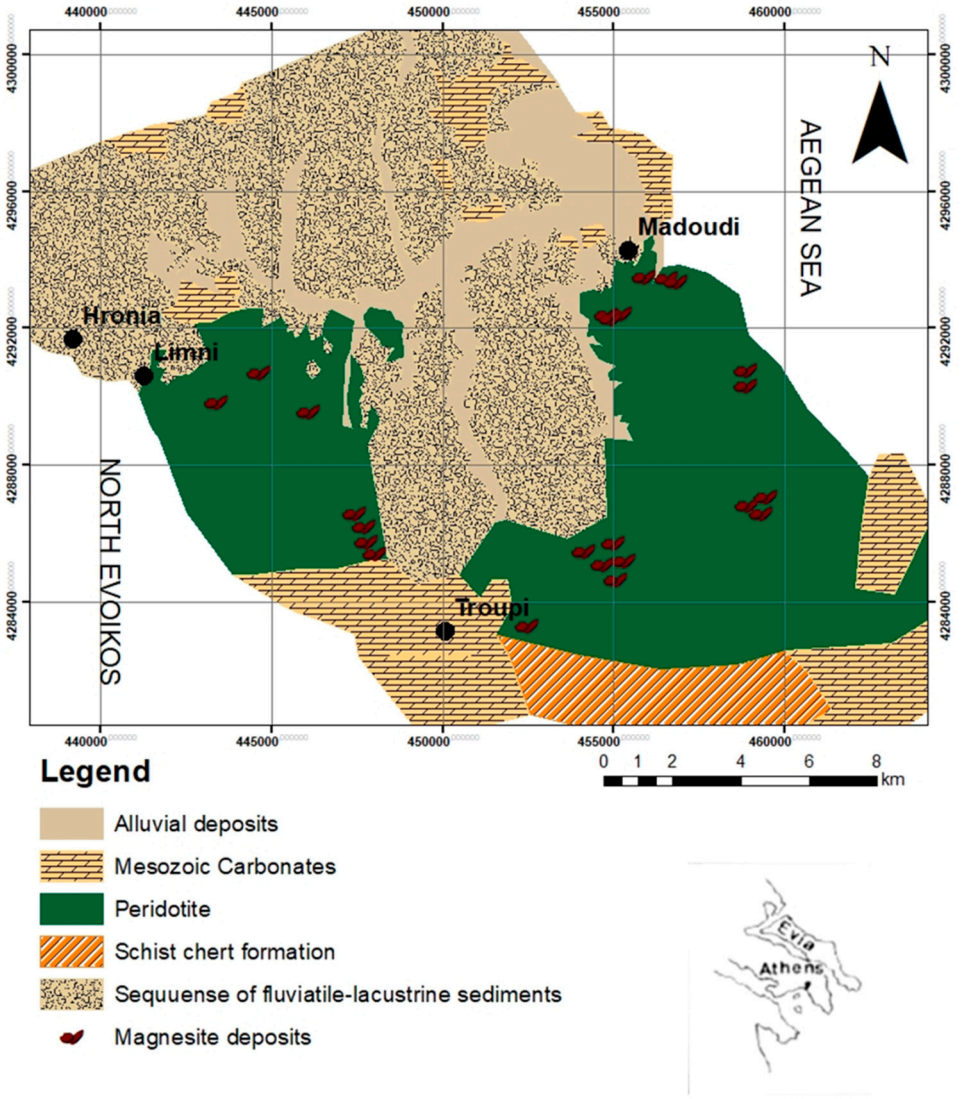

Figure 1. Modified geological map of central and northern Evoia [24] using ArcMap GIS mapping.

3. Materials and Methods

3.1. Materials

In order to investigate the influence of byproducts on the final mortar behavior, providing a new way to solve the environmental pollution of magnesite tailings, magnesite tailings from Evoia (Greece) were collected and used, in order to identify their influence on various produced cements performance. The samples were subsequently crushed, in order to be suitable for all the engineering tests and processing, which were performed according to European and International standards. Additionally, fly ash obtained from a

Kardia lignite-fired power plant in Ptolemais was used in this study in order to investigate its behavior and properties in the produced cements with MEA. Fly ash, along with bottom ash, constitutes the inorganic solid residue after coal combustion. Greek lignite yields, on average, around 30% inorganic content (fly and bottom ash), which is the basic problem because of the enormous amounts produced from lignite combustion. The cement was P·II42.5 Portland cement produced by Titan Co., Ltd. (GREECE). It is a composite cement that completes the range of Portland cements. Its enhanced properties offer high levels of early strength which make it ideal for voluminous concreting and prefabrication work. The used cement was TITAN CEM II 42,5 N which is a composite Portland-type cement with pozzolana/limestone. The pH value of water was 7.0.

3.2. Methods

3.2.1. Methods for Raw Materials

The petrographic features of raw materials were examined using a combination of methods. The mineralogical and textural characteristics of the magnesite tailings were examined in thin sections using a polarizing microscope (Leica Microsystems Leitz Wetzlar, Germany) (University of Patras). The mineralogical composition of the studied samples was determined with X-ray diffraction using a Bruker D8 advance diffractometer with Ni-filtered CuKα radiation. Random powder mounts were prepared by gently pressing the powder into the cavity holder. The scanning area for bulk mineralogy of specimens covered the 2θ interval 2–70°, with a scanning angle step size of 0.015° and a time step of 0.1 s. The mineral phases were determined using the DIFFRACplus EVA 12® software (Bruker-AXS, Fitchburg, MA, USA) based on the ICDD Powder Diffraction File of PDF-2 2006 (University of Patras) while the semi-quantitative calculations were performed by TOPAS 3.0 ® software (TOPAS MC Inc., Oakland, CA, USA), based on the Rietveld method (wt% phase error <1). Morphological texture of raw materials, as well as the chemical composition of minerals, were examined using a scanning electron microscope (SEM) (JEOL JSM-6300 SEM) equipped with an energy dispersive spectrometer (EDS) (Tokyo, Japan). The chemical composition of minerals was determined using natural and synthetic standards and 20 kV accelerating voltage with 10 nA beam current. The samples were carbon-coated to acquire conductance (Forth-ICE-HT, University of Patras). The bulk chemical composition was determined using a Bruker S4-Pioneer XRF wavelength dispersive spectrometer. The spectrometer was fitted with an Rh tube, five analyzing crystals, namely: LIF200, LIF220, LIF420, XS-55, and PET, and the detectors were a gas-flow proportional counter, a scintillation detector, or a combination of the two. Samples were analyzed at 60 kV and 45 mA tube-operating conditions (University of Patras).

The magnesite tailings were crushed by large-, medium-, and small-sized jaw crushers in turn, then milled in a ball mill for 1.0 h. Material retained in each sieve was weighed and expressed as a percentage of the whole sample by using sieves which reached up to 10 μm. The test adopted the method of calcination after briquetting. After stirring 50 g of sieved tailings and 2.0% water and holding the pressure at 6 MPa for 5 s, a cube of 5 cm × 5 cm × 1 cm was made. Then, it was calcined in a box furnace. The calcination was performed on average 1000 °C for 1.0 h, in order for carbonates and/or other clay minerals of tailings to decompose. The calcined tailing was cooled rapidly in the air and passed through a square whole sieve of 0.08 (or 0.1) mm after being milled for 3 min by vibration mill (Western Greece Region, University of Patras).

3.2.2. Methods for the Produced Cement

In order to investigate the consistency and the fluidity of the produced cement specimens, the below process was followed. Based on the mix ratio provided in Equation (1), the test method of cement paste consistency was carried out in accordance with GB/T1346-2011, "Test Methods for Water Requirement of Normal Consistency, Setting Time and Soundness of the Portland Cement". Therefore, the GB/T2419-2005, "Test Method for Fluidity of Cement Mortar", was used. The control sample was composed of 70% ordinary

Portland cement and 30% fly ash. Under dry conditions, nano MgO and fly ash were mixed into the cement to prepare the samples for experiments. The water–binder ratio of all the samples was 0.28. The mixing ratios of the samples are shown in Table 1. Three samples were used for each mix ratio group. The sample size was 25 mm × 25 mm × 280 mm (Western Greece Region).

Table 1. Mixing ratio of cement mortar.

Sample Code	OP Cement	Fly Ash	Nano MgO	Water
Fk1	345	151	0	140
Fk2	340	149	5	140
Fk3	336	147	10	140
Fk4	330	145	15	140
Fk5	325	143	20	140
Fk6	323	141	25	140
Fk7	320	139	30	140
Fk8	310	137	35	140

In order to investigate the expansion of the produced cement specimens, a cuboid of 40 mm × 40 mm × 160 mm was used, with a sand ratio of 1:3 and water cement ratio of 0.5. In order to measure the change of its length, two nail heads were embedded at the end. The substitution rate of fly ash for cement was 0% and 30%, and that of MEA for cement was 0%, 4%, 8%, 12%, and 16%, respectively. The calcination temperature of MEA was 1100 °C, and the holding time was 1 h. The specimen was demolded after standard curing 24 h after forming, and its initial length (L0) was measured after precuring in 20 °C water for 2 h (Western Greece Region). Then, the test pieces were placed into water at 20 °C for long-term curing, and the length (L1) was measured after the corresponding age. The calculation formula of the expansion rate (φ) of the test piece is

$$\varphi = (L1 - L0)/L \quad (1)$$

where L is the effective length of the mortar specimen, taking 150 mm.

The porosity and pore size distribution of mortar were measured by GT-60 mercury intrusion tester produced by Canta Instruments Co., Ltd. (USA) (Western Greece Region).

Regarding the investigation of the compressive strength of the produced cements, three samples were used for each set of mix ratios. The size of the sample was 40 mm × 40 mm × 160 mm. The specimens were cured for 28 and 365 days, autoclave cured, and then their compressive strength and flexural strength were measured. The autoclave curing was performed by curing the sample in a 216 °C and 2.0 MPa saturated steam for 6.0 h after curing in water at 20 °C for 365 days. The model of the autoclave was YZF-2A, which has an inner diameter of 160 mm, volume of 0.0085 m^3, and maximum allowable steam pressure of 25 MPa. The flexural and compressive strengths of the specimens were tested using a compression bending machine and a universal testing machine, respectively. The loading speed of the compressive strength test was controlled at 2.4 ± 0.2 kN/s, and the compressed area of the specimens was 1600 mm^2. The loading speed of the flexural strength test was automatically controlled at 50 N/s. The specimens used for the compressive strength test were adopted after the flexural strength test. The strength of each group of specimens was taken as the arithmetic mean of the measured values of the three specimens (University of Patras).

Atomic force microscopy (AFM) test was taken with digital instruments (University of Patras). AFM height images, including root mean square and roughness, were conducted in order to investigate the morphology of the produced cement.

4. Results and Discussion

4.1. Raw Materials

The MgO content of the magnesite tailings is approximately 40 wt%, while low amounts of silica (5 wt%) and calcium oxides (2.85 wt%) complete the bulk composition (Table 2). The chemistry of this material corresponds to the mineralogical composition of Figures 2 and 3, where magnesite, dolomite quartz, and serpentine were detected. Moreover, the microscopic study using a polarizing and electron microscope assumes the coexistence of magnesite with significant amounts of other crystalline phases. The last reduces the purity in magnesium of the studied materials which is usually demanded for their uses of high economic value (e.g., refractory production). Nevertheless, these wastes are immediately presented clear and free of possible harmful elements.

Table 2. Chemical composition of magnesite tailing (%).

Material	Chemical Compositions						
	CaO	MgO	Al_2O_3	SiO_2	Fe_2O_3	Loss	Total
Magnesite tailing	2.85	40.35	0.03	5.00	0.05	50.75	99.03

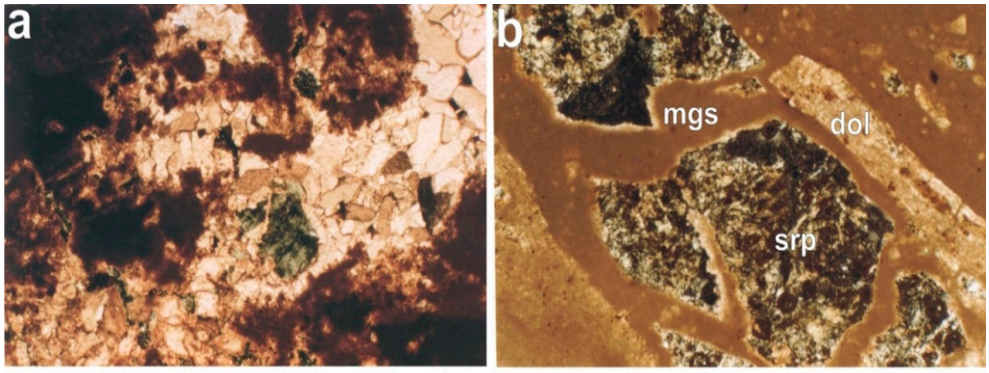

Figure 2. (**a**). Microphotographs where fragments of serpentine (srp), the replacement of magnesite (mgs) by coarse grain dolomite (dol), are observed (XPL, ×68); (**b**) fragments of serpentine in the magnesite vein. In the contact of magnesite with the serpentine fragment, dolomite is formed (XPL, ×68).

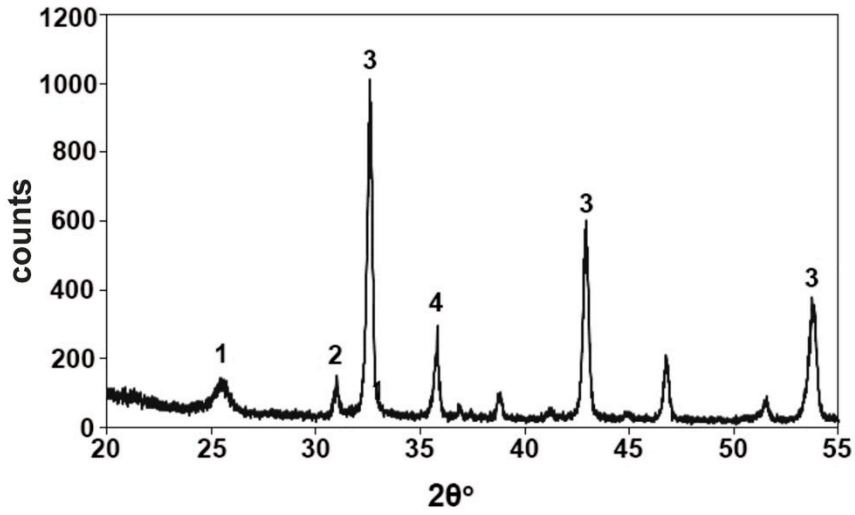

Figure 3. XRD pattern of magnesite tailing from Evoia. 1: quartz, 2: dolomite, 3: magnesite, 4: serpentine.

As it is shown in Figure 2a,b, fragments of serpentine are present in the microstructure of magnesite. Moreover, in Figure 2a, the replacement of magnesite by the coarse grain dolomite can also be observed. In general, the studied magnesite tailings presented are suitable to be used in a variety of applications in which an augmented content of nano MgO is needed.

From the conducted microscopic observation and analyses of the studied tailings, it was shown that although these tailings constitute a rich in magnesium appearance containing over 45% of magnesite, it seems very difficult to obtain a high-quality product (bipolar magnesium) with over 90% MgO. The reason why this happens is due to the nature of this appearance, and more specifically calcium silicate impurities, as are presented in Table 2 and Figure 2. Thus, the mineralogy and the adhesion of the present minerals to the magnesite are responsible for the characterization of the magnesite tailings as a poor appearance for immediate exploitation, despite its MgO content. Magnesite tailings contain in their matrix 79% magnesite, 3% quartz, 3% dolomite, and 15% serpentine (Figure 3). It has been proven that magnesium refractory materials consist of 90% MgO and calcium/SiO_2 ratio of >2.85. In order to use magnesite tailings as refractories, they should contain similar characteristics to those of physical magnesites, such as low content of impurities as CaO, SiO_2, FeO (tot), and B_2O_3, and high amounts of MgO.

This conclusion is obvious as the tailings contain thin veins of serpentine and dolomite and very fine distributed quartz, not only in the dolomite veins, but also in the mass of magnesite. The coexistence of these minerals makes their release very difficult and, therefore, the appearance should be processed and enriched with high-cost processes by spending significant amounts of energy. This is exactly the main reason why these tailings are not easy to use in other applications, something that the present study fully investigates when filling the existing research gaps regarding the use of tailings deriving from magnesites from Greece (as these tailings which are used for the production of environmentally friendly cements have not yet been tested). Additionally, similar raw materials have been used in mortars and have been tested regarding the influence of their MgO content on their final performance [6], where it was found that certain MgO content seems to positively affect the final behavior of the produced mortars. The chemical composition of the used cement is shown in Table 3 and its mineral composition is shown in Figure 4. The main mineral composition of the used cement is C_3S, C_2S, C_3A, and C_4AF, with a small amount of gypsum and bassanite (Figure 4).

Table 3. Chemical compositions of cement (%).

Material	Chemical Compositions									
	CaO	**MgO**	**Al_2O_3**	**SiO_2**	**Fe_2O_3**	**SO_3**	**Na_2O**	**K_2O**	**Loss**	**Total**
Cement	63.16	1.43	4.75	19.47	3.43	2.68	0.28	0.62	3.26	99.08

Nano magnesium oxide is the product produced when the magnesite is heated to 1100 °C; whereupon most of the CO_2 is removed, while 2–7% CO_2 remains, depending on the amount burned [25]. The burned magnesium oxide produced in this study by the thermal decomposition of magnesite at a relatively low temperature, ~1000 °C, is porous, of low bulk density, and chemically active. It is very easily hydrated to $Mg(OH)_2$ or carbonized to $MgCO_3$ even with the humidity or CO_2 of the atmosphere. XRD results indicate the new major phase of periclase to coexist with low amounts of brucite and portlandite (or lime), and the primary remaining magnesite and quartz (Figure 5). The same diffractogram, by its low peak intensities, reveals the fine-grained character of this material. Scarcely, in the microstructure of this calcined product, enriched microregions with the CaO/$Ca(OH)_2$ phases were observed (Figure 6a,b).

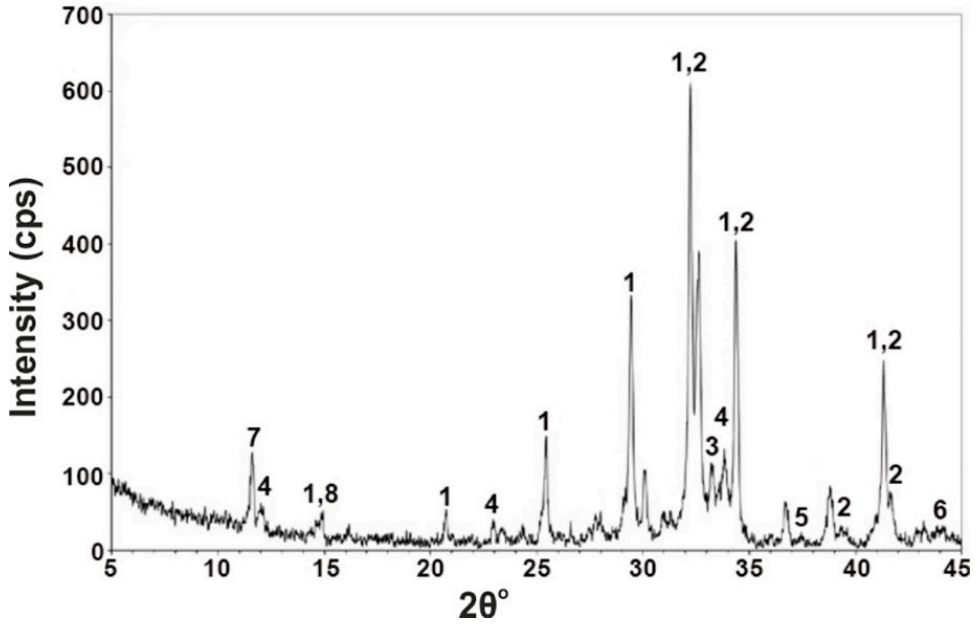

Figure 4. XRD pattern of P 52.5 Portland cement produced by Titan Co., Ltd. (Athens, Greece) where 1: C_3S, 2: C_2S, 3: C_3A, 4: C_4AF, 5: CaO_f, 6:MgO, 7: $CaSO_4$-$2H_2O$-Gypsum, 8: $CaSO_4$ $0.5H_2O$-Bassanite.

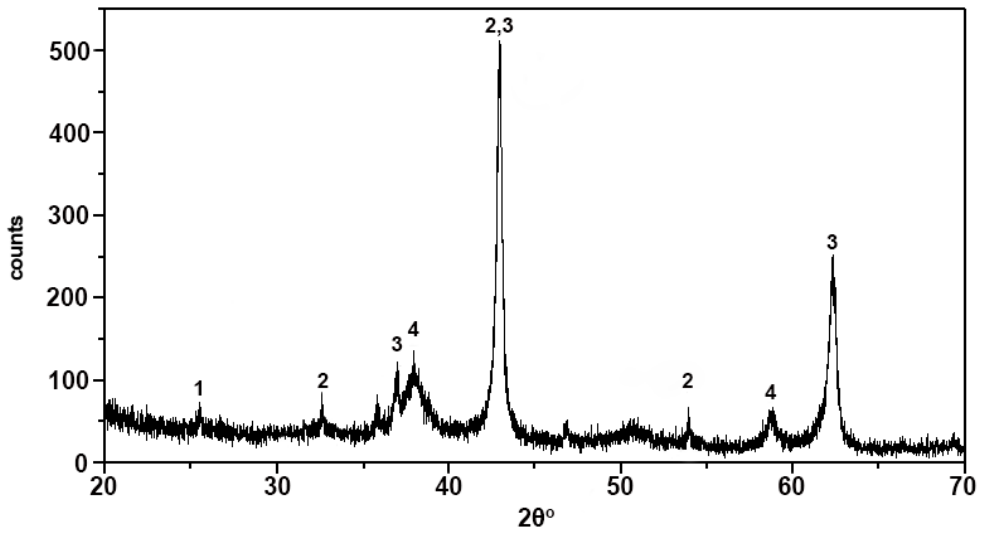

Figure 5. X-ray pattern of bulk mineral composition of final product. 1: Quartz, 2: magnesite, 3: periclase, 4: brucite.

In this study, fly ash was also used, as numerous researchers have used fly ash as an additive for the production of cements of normal and of increased mechanical strength. For this reason, fly ash derived from a Kardia lignite-fired power plant in Ptolemais Basin was collected and studied in order to investigate the behavior and physicomechanical properties of the produced cement in combination with MEA. The characterization of the tested fly ash, which includes mineralogical composition, morphological determination, and chemical composition, revealed that fly ash is enriched in CaO (Table 4). The increased specific surface of its particles makes fly ash capable of restraining elements and participating in chemical reactions due to the microporous minerals included, such as clays and micas [26,27]. Furthermore, the SiO_2 presence constitutes the main carrier of pozzolanic properties, making it useful in cement as an additive. The mineralogical analysis results are shown in Table 3, while powder X-ray diffraction patterns are shown in Figure 7. The basic components of Kardia fly ash are lime, anhydrite, calcite, gehlenite, and less quartz,

plagioclase, and hematite. Micas appear in minor amounts. According to the XRPD results, in the fly ash, amorphous phase ranges to percentages of 25 wt%. Lime anhydrite and quartz appear as the major crystalline phases. Anorthite, portlandite, and gehlenite were also detected in lower amounts.

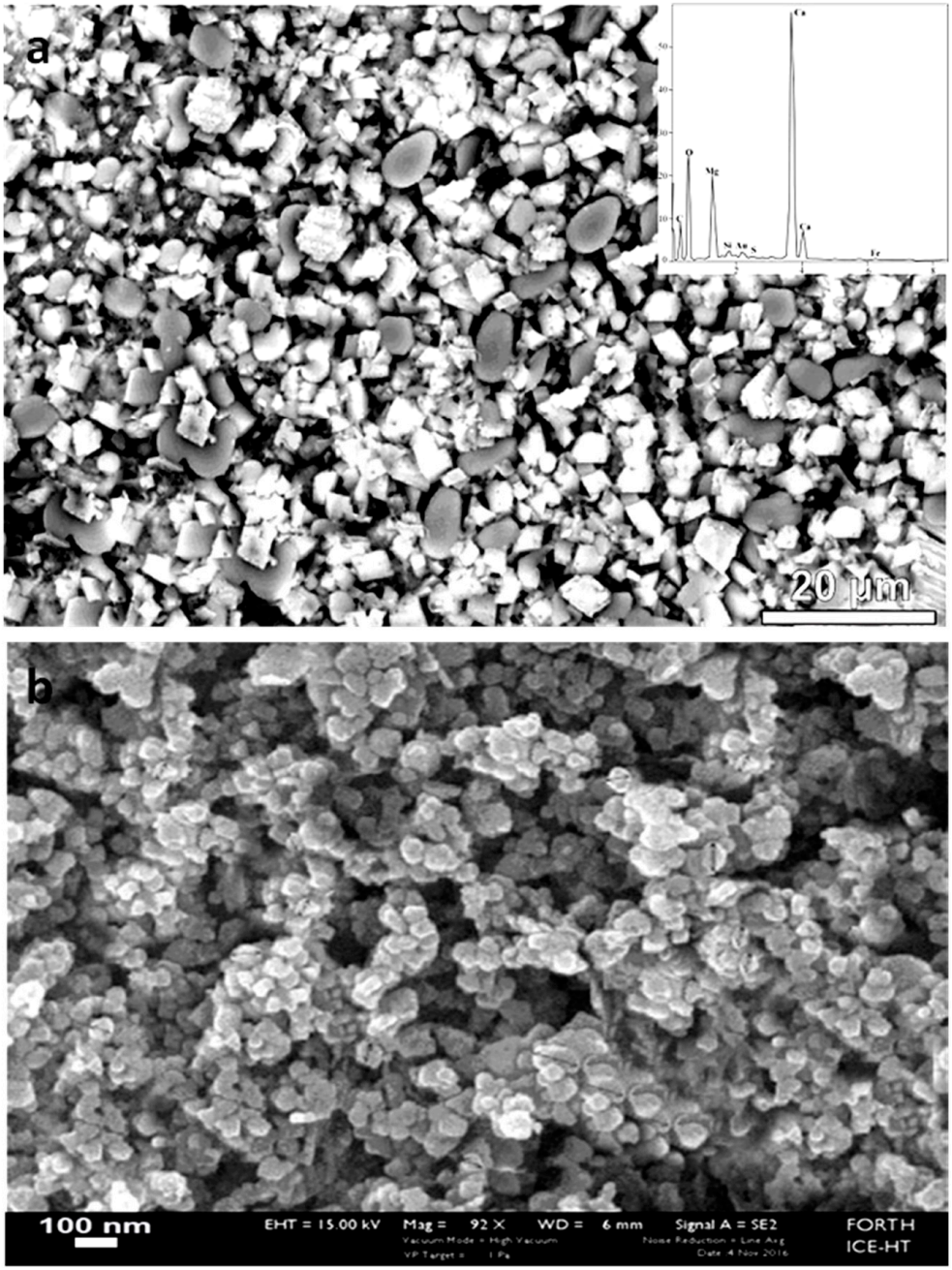

Figure 6. (**a**,**b**) Backscattered image indicating microregion in the matrix of the final product enriched in lime/portlandite (white), and periclase (grey).

Table 5 presents the chemical composition of the investigated fly ash, and the XRD pattern of Figure 7 shows the mineralogical composition of fly ash. The presence of silica dioxide in calcium-rich fly ashes is important even in small amounts [28]. It has been demonstrated that when incorporating high-calcium fly ashes in cementitious systems, the soluble silica present in the ash significantly affects their hydration. Although fly ash rich in active silica is generally more preferable, this does not exclude the possibility of achieving higher reaction rates and superior performance when utilizing different ashes [25]. The

investigated fly ash presents SiO_2 + Al_2O_3 + Fe_2O_3 less than 70% as it is required for Class C classification according to ASTM standards (ASTM 618C) (Table 5). SiO_2 + Al_2O_3 + Fe_2O_3 content also has to be >50%, which is not the case in Greek fly ash due to its high CaO content. However, several authors [25,26] classify Greek fly ash in Class C, taking into consideration the significantly high CaO concentration. It should be mentioned that one major problem regarding fly ash use is the heterogeneity of its chemical composition derived from the chemical composition of feed lignite, the combustion conditions, and the amount of coexcavated inorganic strata that led to combustion. The variability of these factors excludes a constant chemical composition of fly ash for further utilization.

Table 4. Mineral composition (%) of fly ash from a Kardia power plant.

Kardia	
Minerals	**(%)**
Quartz	8
Anhydrite	15
Lime	30
Plagioclase	3
Calcite	14
Gehlenite	10
Hematite	2
Mica	1
Clay minerals	-
Amorphous	17

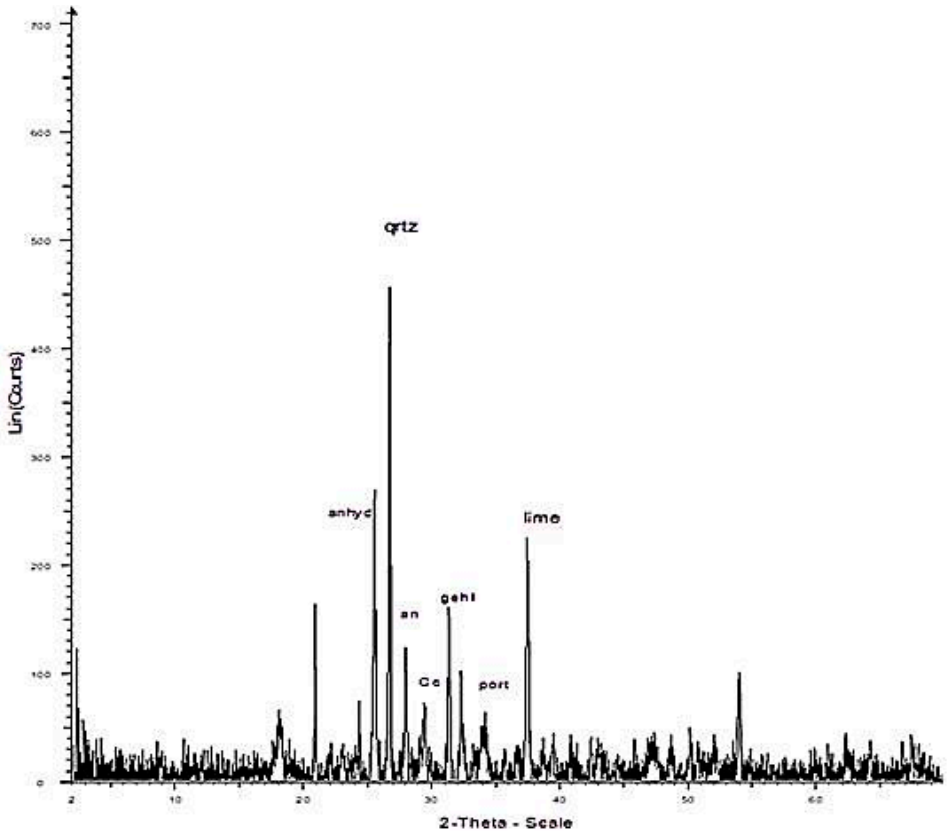

Figure 7. XRD pattern of fly ash from a Kardia power plant: Qrtz: quartz, Cc: calcite, an: anorthite, anhyd: anhydrite, gehl: gehlenite, port: portlandite, lime: lime.

Table 5. Chemical composition (in %) of the fly ash under study (bdl: below detection limit).

Samples	Kardia
Oxides	
CaO	53.00
SiO_2	17.00
Fe_2O_3	12.05
Al_2O_3	5.40
SO_3	8.00
K_2O	2.02
MgO	0.60
TiO_2	1.00
Cr_2O_3	0.19
P_2O_5	0.26
MnO	0.14
SrO	0.09
NiO	0.09
Na_2O	Bdl
ZrO_2	0.06
CuO	0.04
ZnO	0.03
Rb_2O	0.02

As for the morphological features of the tested fly ash, properties of plerospheres, cenospheres (hollow spheres), and agglomerates, which result from lignite combustion, were observed. A plerosphere constitutes a cenosphere that may encapsulate a mass of microspheres and is generally silica-coated (Figure 8a–c).

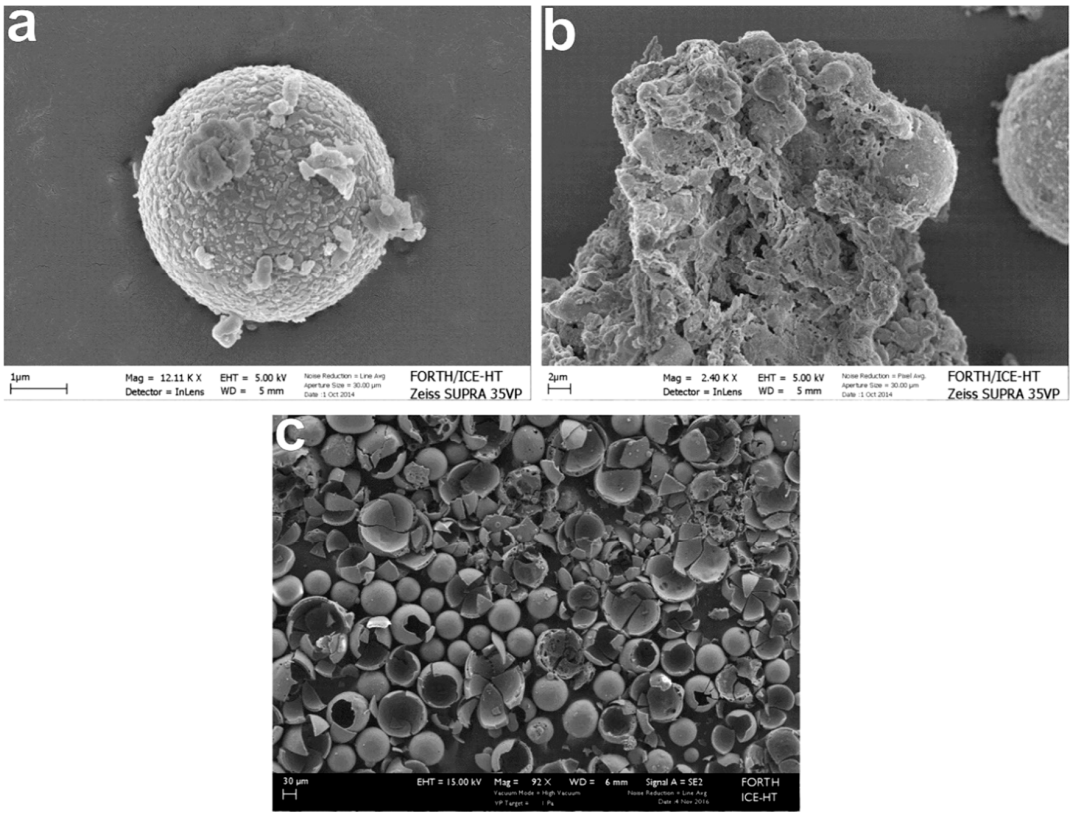

Figure 8. Fly ash particles from a Kardia power plant: (**a**–**c**): Cenospheres after releasing their gases, silica-coated perfect sphere, and with smaller particles on its surface.

The authors, after having taken into account the above results of the used raw materials, concluded that the raw materials are individually suitable to be used as raw materials for cement production of high mechanical, as well as of high physical, characteristics. Each of the basic components of cement exhibits a capable behavior, as it is shown that by varying their relative percentages, the properties of cement can be modified. Similar raw materials have been investigated and tested by numerous researchers to be used as cement additives and they are considered as suitable for this type of application. However, the exact proportions of raw materials used in order to produce such green applications has not been identified yet and is something that this study investigates.

4.2. Factors Influencing the Behavior of the Products

MEA is typically produced by calcining magnesite at a temperature ranging from 900 °C to 1200 °C, which is much lower than the cement clinker temperature, and as a result provides higher hydration reactivity in comparison to the dead burnt periclase. In this study, MEA was used after its calcining in 1100 °C by staying at this temperature for one hour and was mixed with fly ash to study their effect on the final behavior of the produced cements (Figure 6). The mineral composition analysis results of MEA produced by calcining magnesite tailings at 1100 °C for 1.0 h, presented in Figure 5, and the comparison of minerals before and after calcination, in Figures 3 and 5, when the calcination temperature and holding time were up to 1100 °C for 1 h, show that carbonate and clay minerals were decomposed, or only a trace amount could not be displayed on the XRD pattern (Figure 5). In addition, the XRD pattern shows that the main minerals obtained after 1 h of heat preservation were periclase (MgO), as well as small amounts of portlandite, brucite, and initial quartz. This mineralogical modification during calcining appears to have a significant effect on the activity and expansion performance. This is exactly shown by the diagram of Figure 9, which shows that a small percentage of calcining magnesite tailings at 1100 °C for 1.0 h performs satisfactorily.

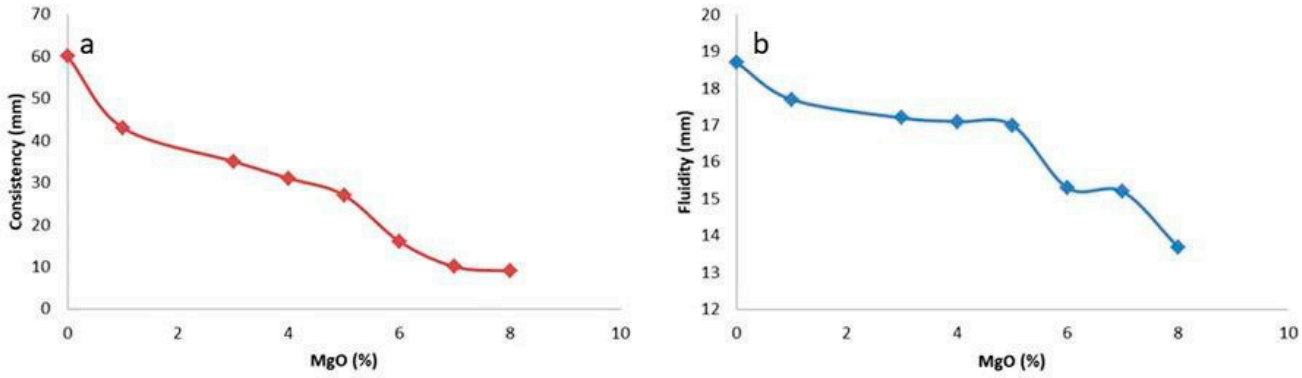

Figure 9. Influence of MgO on the (**a**) consistency and (**b**) fluidity of cement.

4.2.1. The Effect of Nano MgO on the Consistency of the Produced Cement

The influence of nano MgO, as well as of fly ash in certain contents, as they are displayed in Table 1, seems to be intensively strong for the total of the tests of the produced cement. However, the most significant influence presented is the nano MgO content. The effect of nano MgO on the consistency of the produced cement paste is presented in Figure 9a. The observation of this figure shows that the increased amount of nano MgO results in the gradual decrease of its consistency. Several researchers have reached similar conclusions [14,28]. In the case that the content of nano MgO was 1%, the sinking depth of the test cone was 42 mm, while when the content of nano MgO was 3%, the consistency of cement was 35 mm. When the content of nano MgO was more than 4%, the consistency value of the specimen decreased more significantly.

The general behavioral trend of the studied mixtures could be defined into three (3) different groups regarding the total of their properties, as is presented in Figure 9a,b. It

can be observed that group I consists of FK1 and FK2 samples, group II of FK3–FK5, and group III of FK6–FK8. This discrimination of clear limits reveals that there are certain critical values of MgO and fly ash content which determine the final cement properties. When studying the diagrams of Figure 1 combined with Table 1, and knowing the raw materials used as waste materials of other processes (tailings) and fly ash, it was observed that high content of fly ash (Kardia, Greece) combined with low content of MgO provides high values of consistency and fluidity, and, on the other hand, low content of fly ash and high content of nano MgO provides lower values in consistency and fluidity; something that seems to be defined mainly by the nano MgO content and, more specifically, by their hydration activity.

4.2.2. The Effect of Nano MgO on the Fluidity of the Produced Cement

The way in which the fluidity of the produced cement was influenced by the content of nano MgO is depicted in the diagram of Figure 9b, and as is shown in this figure, the nano MgO content plays a severe role. It can be observed that by the increase of nano MgO content, the fluidity is decreased almost linearly, which is consistent with the law of cement paste consistency. Xiaoyan Wang [29] investigated the effect of nano MgO on the fluidity of oil-well cement paste and found a similar phenomenon. The effect of nano MgO content on the fluidity of cement paste was relatively obvious, and the fluidity of cement paste decreased with the increase in nano MgO content. When the nano MgO content was 1.0%, the fluidity of the oil-well cement slurry worsened because the water demand of nano MgO increased and generated $Mg(OH)_2$, which also caused the consistency of the cement paste to become worse. The nano MgO has a small bulk density, which may affect the bulk density of the freshly mixed specimens. Therefore, it may disrupt the uniform particle assembly. Furthermore, it has a large specific surface area and high hydration activity, and as a result, it reacts with water rapidly. In fresh cement paste, nano MgO consumed more free water for hydration and covering its surface layer [30–32], thus reducing the water–cement ratio and leading to reduced fluidity and consistency. Xue Zhang found that when a high-MgO admixture of cement was used or excess MgO was used to mix high-performance concrete, a higher water–solid ratio was required [33,34]. Ye et al. [35], when studying the performance of cement-based materials made by cement paste, including nano MgO oxide and fly ash deriving from their surrounding areas, found similar trends to the results of our study which contains cements made by nano MgO oxides and fly ash deriving from Greece.

4.2.3. The Effect of Nano MgO on the Expansion of the Produced Cement

In the present study, the ability of cement paste to expand was examined, as it is a particularly important parameter of its basic characteristics. The present experimental study used numerous samples for a significant period of time up to 400 days, making a systematic study of the raw materials which showed that a specific content of nano MgO and fly ash in powder as specific additives can be decisively active in the controlled shrinkage and expansion of the cement. This achieves the desired degree of volume dimension, while compensating for the shrinkage effects, avoiding the volume shrinkage of the cement. The present raw materials, as they do not present metallic elements, are not feasible and will affect any future Fe reinforcements. Its dilating action seems to begin in the first 8 days and ends depending on the ratio of nano MgO/fly ash from 8 to 400 days. Samples containing low percentage of MgO immediately complete their expansion, while mixtures with an increased percentage in nano MgO continue to evolve 400 days later. The expansion of the cement paste has been remarkably improved due to the nano MgO addition; nevertheless, the accurate limits of the MgO content added have not yet been defined. The expansion performance increases as the nano MgO content increases, following the extension of the curing age. Firstly, the expansion of the cement paste containing nano MgO oxide was significantly higher than that of the cement paste without MgO oxide. This may have happened because the nano MgO particles were small, and $Mg(OH)_2$ crystals were quickly

formed due to hydration, and as a result, this gives higher expansion to the cement paste. Furthermore, $Mg(OH)_2$ crystals grow around the pore rims and near the MgO particles, and the increased volume of $Mg(OH)_2$ crystals squeezes the surrounding cement paste and causes expansion [6,30,35,36]. The expansion of the tested cement paste samples are presented in Figure 10. As can be observed from the diagram (Figure 10), as the nano MgO rises, the expansion increases. The expansion of the sample without nano MgO was 364 μm/m after autoclave curing, while the expansion amounts were 1060, 1700, 2500, 3300, and 4000 μm/m when nano MgO was 4, 5, 6, 7, and 8%, respectively, after autoclave treatment. Several scientists have obtained similar results [6,35]. It is worth mentioning that in the expansion test, a clear discrimination among the three groups is observed, characterized by clear limits in the used mixtures of nano MgO/fly ash. In the present systematic study of the effect of additives on the behavior of the produced cement, representative samples from the two groups were studied, giving the most satisfactory results in order to identify the effect of raw materials on the final behavior of cement.

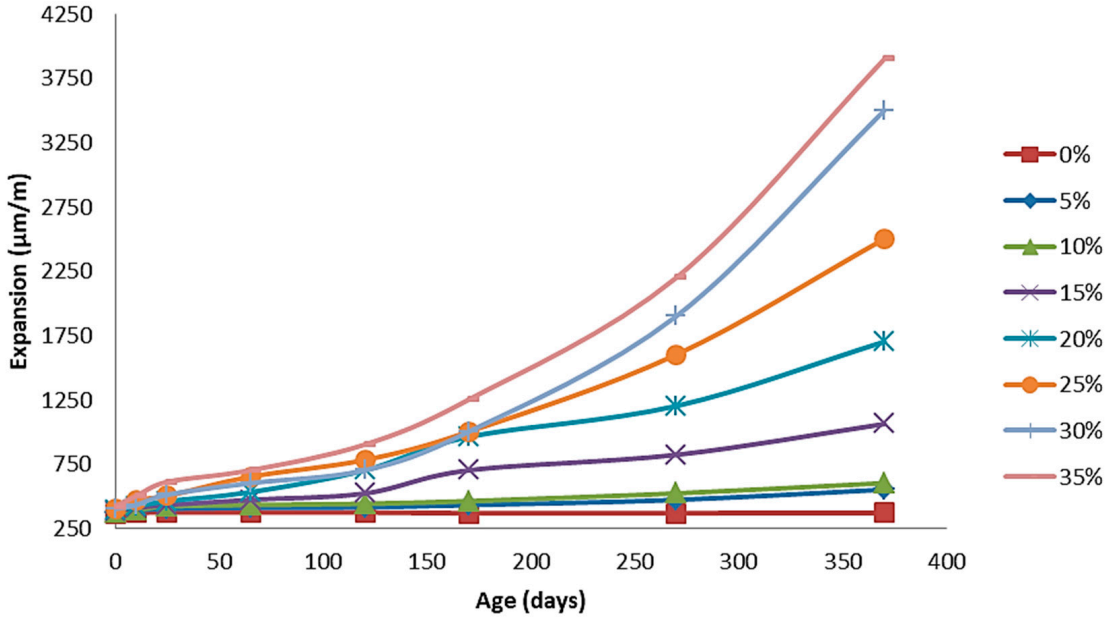

Figure 10. Effect of nano MgO content on expansion performance of cement paste.

4.2.4. The Effect of Nano MgO/Fly Ash on the Cement Porosity

As shown in Figure 11, we observed different pore distribution in the cement paste directly depending on the content of nano MgO/fly ash. Pore distribution and total porosity are factors that affect the final strength, permeability, and volume changes in the hardened cement paste. The pore size distribution and porosity of cement paste is affected by the nano MgO, as can be seen in Figure 11. The total porosity of the cement decreased as the curing age increased. The porosity of the produced cement containing 8% of nano MgO oxide was higher than that of cement containing 4% of nano MgO oxide, which may be due to the excessive content of nano MgO oxide, which led to harmful expansion and increased the harmful pore size of mortar. This observation may be due to the presence of MgO as well as the process of MgO hydration; there are three main stages that may occur at the same time but can be dominant at different times. In the first two stages, reactive nano MgO particles dissolve and leave pores in the whole system, and then minor $Mg(OH)_2$ crystals grow freely to fill these pores without generating crystal growth pressure. The third stage is dominated by confined crystallization, and expansion is mainly caused by microcracks induced by the crystal growth pressure in the whole system. Hydration of MgO makes the pore structure partially dense or increases the tortuosity of pores, which will improve durability; furthermore, if high expansion occurs, high porosity will reduce

durability. The strength of hardened cement is considered to be its most important property. Each of the basic components of cement presents a specific behavior where, by varying their relative percentages, the mechanical properties of the cement can be modified. It should also be noted that as the total porosity of the cement decreased as the curing age increased, the cement became denser, and the strength became higher. This is exactly what is shown in Figure 12, where the division into three groups with clear boundaries of specific ratios of nano MgO/fly ash is clearly shown. The clear separation of the three groups, from the beginning of the study, with the factors affecting the cement is obviously shown in Figure 12, which is directly related to the total of the results given so far. For example, the differentiation of the two groups in terms of porosity and its distribution (Figure 11) is in complete agreement with the groups of Figure 12, and the distribution of pores is affected by the ratio of water to cement and the degree of hydration of the cement. Large pores (>50 nm) affect the compressive strength, while smaller ones have a greater effect on drying shrinkage and creep.

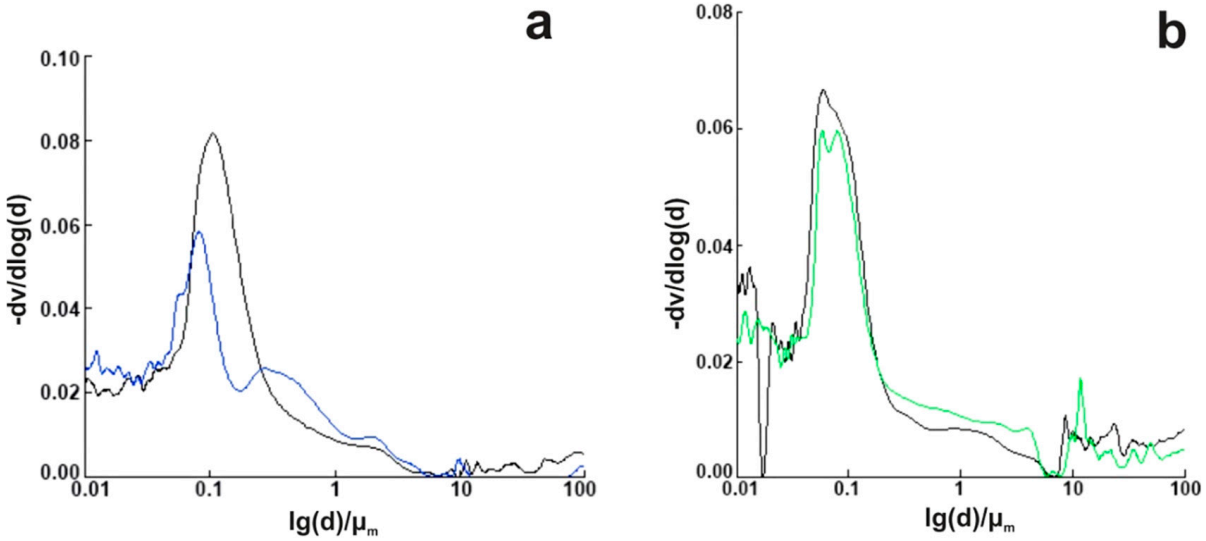

Figure 11. Pore size distribution of mortars containing MEA: (**a**) 4% MEA; (**b**) 8% MEA.

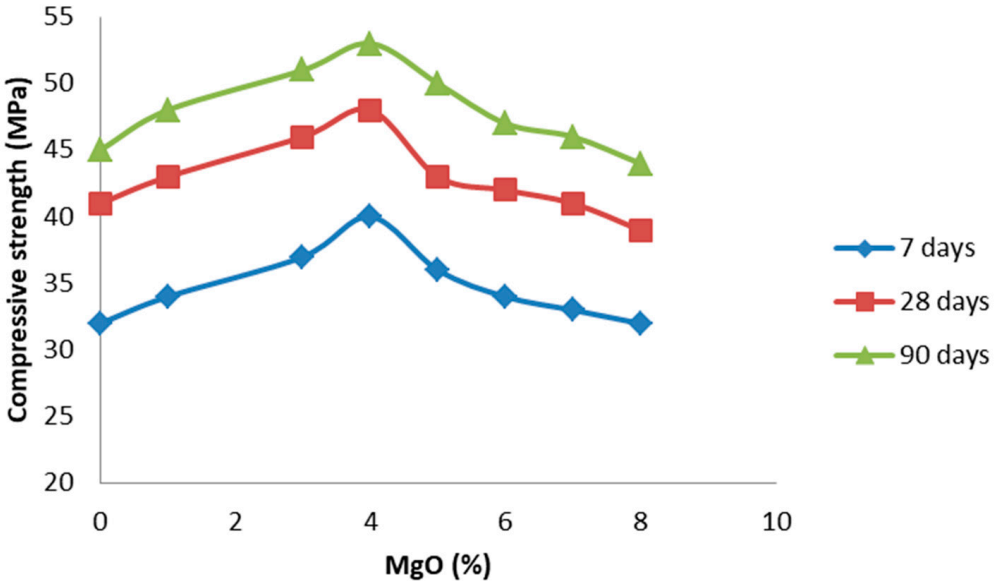

Figure 12. The compressive strength of cement paste samples with MgO.

4.2.5. The Effect of Nano MgO on the Mechanical Performance of the Produced Cement

Moreover, the physical interpretation of the diagrams of Figures 9 and 10 is harmonious with the final behavior and strength of the hardened cement directly dependent on the mineral raw materials, where they participate in the composition of the cement (Table 1). In general, the cement strength seems to show increasing trends in the tests of 7, 28, and 90 days for contents of nano MgO up to 4% of the volume of cement, probably because the microstructure improved after nano MgO incorporation. With the extension of the curing age, the compressive strength of all samples gradually increased, most likely because fly ash underwent a pozzolanic reaction, which improved the interface transition zone of the cement [37]. However, we can observe that when the content of MgO was up to 4%, the compressive strength values, regardless of the curation days, show reducing trends, which is probably due to the development of a strong network of microcracks in the structure of the mortar, displaying its properties. We found similar conclusions from the test of expansion. In addition, hydration of C–S–H in these critical samples seems to have been accelerated, leading to the loss of cohesive forces within the cement structure.

4.2.6. The Effect of Microroughness on the Cement Performance

The AFM technique constitutes a very useful tool for examining the surface morphology of various materials such as cement. The initial grouping into three subgroups is also verified by the study of the microroughness of the cements through the AFM method. As shown in Figure 13, the samples of group I, representing the lowest percentage in MEA, show low microroughness and therefore may constitute a determining factor in the low cohesion of the cement paste, as the microtopography is likely to create limited development of cohesive forces within the structure of the cement paste. In contrast to the above, in group II, there is increased microroughness due to the increase in the size of MEA, where it creates increased cohesive forces within the cement paste. This increase in the microroughness, in addition to the mechanical cohesion, is likely to create additional van der Waals forces between the nano MgO and the cement minerals due to this increase in the specific surface area. Finally, group III is presented with a particularly high microroughness compared to the previous groups. However, this increase seems to overcome the mechanical forces and the van der Waals forces, so it breaks into bonds, creating a number of microcracks. This is supported by both the results of the uniaxial compressive strength and the petrographic study of the produced cements.

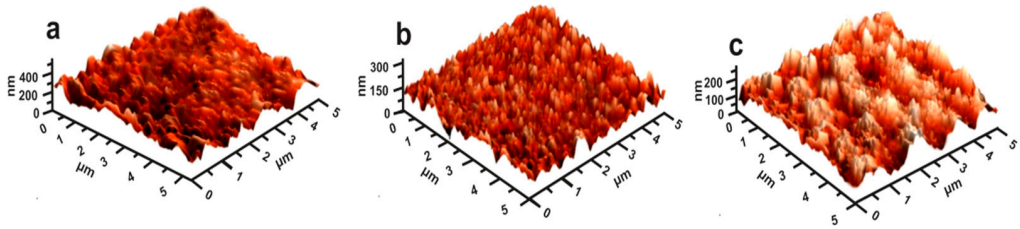

Figure 13. The AFM results of cement made by nano MgO and fly ash additives: (**a**), group I, (**b**) group II, (**c**) group III.

5. Conclusions

This paper examines byproducts (magnesite tailings and fly ash) to evaluate their suitability as cement additives, with the ultimate goal of the production of environmentally friendly cements from now on. The main conclusions of this study are given in the below remarks:

- Byproducts from different regions of Greece, such as magnesite tailings from Evoia and fly ash from Kardia (Ptolemais), which have been combined together for first time, are suitable reinforcement additives.
- The effect of nano MgO content is the most critical parameter for the physicomechanical performance of produced cement, compared to that of the fly ash content.

- More satisfactory results in the physicomechanical properties of the produced cement were from samples of group II, containing 3–4% of nano MgO. Nano MgO content above 4% seems to have a negative influence on the compressive strength of the produced cement, simultaneously reducing its durability. Therefore, the amount of nano MgO determines the physicomechanical performance of the produced cement.
- The increased microroughness of the cements is in accordance with the mechanical behavior of the produced cements.

Future scope: Our research team, following the basic principles of the circular economy, aims to produce a green concrete in the future using exclusively industrial byproducts for both cement and aggregates in mixtures capable of withstanding uniaxial loads and temperature changes.

Author Contributions: Conceptualization, P.P.G. and P.P.; methodology, P.P.G., P.P., A.R., P.L. and M.K.; software, M.K. and P.P.; investigation, P.P.G., P.P., A.R. and P.L.; resources, P.P.G., P.P. and P.L.; data curation, P.P.G., P.P., A.R. and P.L.; writing—original draft preparation, P.P.G. and P.P.; writing—review and editing, P.P.; visualization, P.P.; supervision, P.P. All authors have read and agreed to the published version of the manuscript.

Funding: This research received no external funding.

Institutional Review Board Statement: Not applicable.

Informed Consent Statement: Not applicable.

Conflicts of Interest: The authors declare no conflict of interest.

Abbreviations

AFM	Atomic force microscopy
ASTM	International standards worldwide
dol	Dolomite
EDS	Energy dispersive spectrometer
MEA	MgO expansion agent
mgs	Magnesite
OP	Ordinary Portland
PC	Portland cement
srp	Serpentine
XRD	X-ray diffraction
XRF	X-ray fluorescence
XRPD	X-ray powdered diffraction

References

1. Freedonia. World Construction Aggregates-Demand and Sales Forecasts, Market, Share, Market, Size, Market, Leaders. In *Industry Study No. 3389*; The Freedonia Group: Cleveland, OH, USA, 2016; p. 390.
2. USGS. Commodity Statistics and Information Mineral. In *Yearbooks*; USA Geological Survey: Washington, DC, USA, 2015.
3. Petrounias, P.; Rogkala, A.; Giannakopoulou, P.P.; Lampropoulou, P.; Xanthopoulou, V.; Koutsovitis, P.; Koukouzas, N.; Lagogiannis, I.; Lykokanellos, G.; Golfinopoulos, A. An Innovative Experimental Petrographic Study of Concrete Produced by Animal Bones and Human Hair Fibers. *Sustainability* **2021**, *13*, 8107. [CrossRef]
4. Petrounias, P.; Giannakopoulou, P.P.; Rogkala, A.; Lampropoulou, P.; Tsikouras, B.; Rigopoulos, I.; Hatzipanagiotou, K. Petrographic and Mechanical Characteristics of Concrete Produced by Different Type of Recycled Materials. *Geosciences* **2019**, *9*, 264. [CrossRef]
5. José, N.; Ahmed, H.; Miguel, B.; Luís, E.; Jorge, D.B. Magnesia (MgO) Production and Characterization, and Its Influence on the Performance of Cementitious Materials: A Review. *Materials* **2020**, *13*, 4752. [CrossRef]
6. Ye, Y.; Liu, Y.; Shi, T.; Hu, Z.; Zhong, L.; Wang, H.; Chen, Y. Effect of Nano-Magnesium Oxide on the Expansion Performance and Hydration Process of Cement-Based Materials. *Materials* **2021**, *14*, 3766. [CrossRef]
7. Shayanfar, M.A.; Farnia, S.M.H.; Ghanooni-Bagha, M.; Massoudi, M.S. The Effect of Crack Width On Chloride Threshold Reaching Time in Reinforced Concrete Members. *Asian J. Civ. Eng.* **2020**, *21*, 625–637. [CrossRef]
8. Jackson, N. *Civil Engineering Materials*; Macmillan Press Ltd.: London, UK, 1981.
9. Neville, A.M. *Properties of Concrete, ELSB*, 5th ed.; Pearson Education Publishing Ltd.: London, UK, 2005.

10. Kabir, H.; Hooton, R.D. Evaluating Soundness of Concrete Containing Shrinkage-Compensating MgO Admixtures. *Constr. Build. Mater.* **2020**, *253*, 119141. [CrossRef]
11. Ye, Q.; Chen, H.; Wang, Y.; Wang, S.; Lou, Z. Effect of MgO and gypsum content on long-term expansion of low heat Portland slag cement with slight expansion. *Cem. Concr. Compos.* **2004**, *26*, 331–337. [CrossRef]
12. Lou, Z.; Ye, Q.; Chen, H.; Wang, Y.; Shen, J. Hydration of MgO in clinker and its expansion property. *J. Chin. Ceram. Soc.* **1998**, *26*, 430–436. [CrossRef]
13. Walling, S.; Provis, J. Magnesia-based cements: A journey of 150 years, and cements for the future? *Chem. Rev.* **2016**, *116*, 4170–4204. [CrossRef] [PubMed]
14. Liu, Z.; Wang, S.; Huang, J.; Wei, Z.; Guan, B.; Fang, J. Experimental Investigation on the Properties and Microstructure of Magnesium Oxychloride Cement Prepared with Caustic Magnesite and Dolomite. *Constr. Build. Mater.* **2015**, *85*, 247–255. [CrossRef]
15. Dimopoulos, I.; Anastassakis, G. Recovery of magnesite from fine waste material rejected before hand-sorting. In Proceedings of the XV Balkan Mineral Processing Congress, Sozopol, Bulgaria, 12–16 June 2013; Volume 1, pp. 213–216.
16. Martek, I.; Hosseini, M.R.; Shrestha, A.; Edwards, D.J.; Durdyev, S. Barriers inhibiting the transition to sustainability within the Australian construction industry: An investigation of technical and social interactions. *J. Clean. Prod.* **2019**, *211*, 2812–2892. [CrossRef]
17. Kuppig, V.D.; Cook, Y.C.; Carter, D.A.; Larson, N.J.; Williams, R.E.; Dvorak, B.I. Implementation of sustainability improvements at the facility level: Motivations and barriers. *J. Clean. Prod.* **2016**, *139*, 15291–15538. [CrossRef]
18. Murtagh, N.; Scott, L.; Fan, J.L. Sustainable and resilient construction: Current status and future challenges. *J. Clean. Prod.* **2020**, *268*, 10. [CrossRef]
19. Vishwakarma, V.; Uthaman, S. Environmental impact of sustainable green concrete. In *Smart Nanoconcretes and Cement-Based Materials: Properties, Modelling and Applications*; Elsevier: Amsterdam, The Netherlands, 2019; pp. 241–255.
20. Robertson, A.H.E. Origin and emplacement of an inferred late Jurassic subduction-accretion complex, Euboea, eastern Greece. *Geol. Mag.* **1991**, *128*, 27–41. [CrossRef]
21. Katsikatsos, G. *Geological Map, Sheet LIMNI*; Scale 1:50.000,1.G.M.E.; Institute of Geology and Mineral Exploration: Athens, Greece, 1980.
22. Spray, J.G.; Roddick, J.C. Petrology and 40Ar/39Ar Geochronology of some Hellenic Sub-Ophiolite Metamorphic Rocks. Contrib. *Mineral. Petrol.* **1980**, *72*, 43–55. [CrossRef]
23. Thuizat, R.; Whitechurch, H.; Montigny, R.; Juteau, T. K-Ar dating of some infra-ophiolitic metamorphic soles from the Eastern Mediterranean: New evidence for oceanic thrustings before obduction. *Earth Planet. Sci. Lett.* **1981**, *52*, 302–310. [CrossRef]
24. Gartzos, E. Carbon and oxygen irotope constraints on the origin of magnesite deposits, North Evia (Greece). *Schweiz. Mineral. Petrogr. Mitt.* **1990**, *70*, 67–72.
25. Mehta, P.K. Pozzolanic and cementitious byproducts as mineral admixtures for concrete—-A critical review. In Proceedings of the 1st International Conference on the Use of Fly Ash, Silica Fume, Slag, and Natural Pozzolans in Concrete, ACI SP-79, Detroit, MI, USA, July 1983; p. 1.
26. Rai, P.; Qiu, W.; Pei, H.; Chen, J.; Ai, X.; Liu, Y.; Ahmad, M. Effect of Fly Ash and Cement on the Engineering Characteristic of Stabilized Subgrade Soil: An Experimental Study. *Geofluids* **2021**, *2021*, 1–11. [CrossRef]
27. Koukouzas, N.K.; Zeng, R.; Perdikatsis, V.; Xu, W.; Kakaras, E.K. Mineralogy and geochemistry of Greek and Chinese coal fly ash. *Fuel* **2006**, *85*, 2301–2309. [CrossRef]
28. Gao, P.; Lu, X.; Geng, F.; Li, X.; Hou, J.; Lin, H.; Shi, N. Production of MgO-type Expansive Agent in Dam Concrete by Use of Industrial By-Products. *Build. Environ.* **2008**, *43*, 453–457. [CrossRef]
29. Wang, X. Investigations of Nano-Materials Modified Cement Slurry(Stone) Structure and Properties. Master's Thesis, China University of Petroleum, Beijing, China, 2016; pp. 37–38.
30. Ding, W. Study on the Properties of Cement Paste and Mortar with MgO Expansive Admixture. Master's Thesis, Southwest University of Science and Technology, Mianyang, China, 2016; pp. 36–37.
31. Mo, L.; Deng, M. Thermal behavior of cement matrix with high-volume mineral admixtures at early hydration age. *Cem. Concr. Res.* **2006**, *36*, 1992–1998.
32. Mo, L.; Min, D.; Tang, M. Effects of calcination condition on expansion property of MgO-type expansive agent used in cement-based materials. *Cem. Concr. Res.* **2010**, *40*, 437–446. [CrossRef]
33. Zhang, X. Microscopic Characterization and Early age Performance of MgO and Nano MgO High Performance Concrete. Master's Thesis, Shandong University, Jinan, China, 2019; pp. 33–34.
34. Ding, W.; Tan, K.; Liu, L.; Tang, K.; Zhao, C. Influence research of light-burned magnesia on autogenous shrinkage and pore structure of steam-cured cement paste. *China Concr. Cem. Prod.* **2016**, *5*, 21–26.
35. Ye, Q.; Yu, S.; Zhang, Z.; Zhang, Q.; Shi, T. Effect of Nano-MgO on the expansion and strength of hardened cement paste. *J. Build. Mater.* **2017**, *20*, 765–769.
36. Zhou, L.; Wang, Y.; Zhang, G.; Zhang, F. Research progress in the effect of Nano-MgO on the properties of cement-based materials. *China Concr. Cem. Prod.* **2019**, *5*, 13–18.
37. Chen, H. Expansive property and pore structure characterisitics of magnesium oxide slight expansive cement- fly ash binding material. *J. Chin. Ceram. Soc.* **2005**, *33*, 516–519.